

# Multilevel Second-Moment Methods with Group Decomposition for Multigroup Transport Problems

Dmitriy Y. Anistratov<sup>a,b</sup>, Joseph M. Coale<sup>a,c</sup>, James S. Warsa<sup>d,e</sup>, Jae H. Chang<sup>d,f</sup>

<sup>a</sup>*Department of Nuclear Engineering, North Carolina State University Raleigh, NC*

<sup>b</sup>*anistratov@ncsu.edu*

<sup>c</sup>*jmcoale@ncsu.edu*

<sup>d</sup>*Los Alamos National Laboratory, Los Alamos, NM 87545, USA*

<sup>e</sup>*warsa@lanl.gov*

<sup>f</sup>*jhchang@lanl.gov*

## Abstract

This paper presents multilevel iterative schemes for solving the multigroup Boltzmann transport equations (BTEs) with parallel calculation of group equations. They are formulated with multigroup and grey low-order equations of the Second-Moment (SM) method. The group high-order BTEs and low-order SM (LOSM) equations are solved in parallel. To further improve convergence and increase computational efficiency of algorithms Anderson acceleration is applied to inner iterations for solving the system of multigroup LOSM equations. Numerical results are presented to demonstrate performance of the multilevel iterative methods.

*Keywords:* particle transport, Boltzmann equation, multigroup problems, iterative methods, parallel algorithms, Anderson acceleration

## 1. Introduction

The steady-state energy-dependent particle transport problems are formulated by the multigroup Boltzmann transport equation (BTE) given by

$$\boldsymbol{\Omega} \cdot \nabla \psi_g(\mathbf{x}, \boldsymbol{\Omega}) + \sigma_{t,g}(\mathbf{x}) \psi_g(\mathbf{x}, \boldsymbol{\Omega}) = \frac{1}{4\pi} \sum_{g'=1}^G \sigma_{s,g' \rightarrow g}(\mathbf{x}) \int_{4\pi} \psi_{g'}(\mathbf{x}, \boldsymbol{\Omega}') d\boldsymbol{\Omega}' + \frac{1}{4\pi} Q_g(\mathbf{x}), \quad g \in \mathbb{G}, \quad (1)$$

where  $\mathbb{G} = \{1, \dots, G\}$ . Here standard notation is used. This equation models interaction of particles with matter in a physical system with absorption and isotropic scattering. It has application for linear transport problems of various kind of particles, for instance, neutrons, electrons, and photons. In nonlinear thermal radiative transfer (TRT) problems, the time-dependent BTE is coupled with the material energy balance (MEB) equation. A group of methods for TRT is based on linearization of the system of equations on a time step. This reduces the TRT problem to the BTE equation of the form (1) with pseudo-scattering [1, 2, 3].

Numerical transport algorithms for high performance computers use a variety of approaches to achieve efficient parallel computations for solving the linear BTE [4, 5]. A natural element of parallel algorithms is to perform calculations of group equations in parallel taking advantage of the particle transport problem’s multigroup structure. This can be interpreted as problem decomposition over one element of the phase space, namely, particle energy. Efficient Diffusion Synthetic Acceleration (DSA) algorithms for multigroup transport problems can be formulated with decoupled group equations [6].

In this paper, we describe new iterative methods for multigroup transport problems which solve the group equations in parallel. They are formulated on the basis of low-order equations of the Second-Moment (SM) method and nonlinear projective approach [7, 8, 9]. The low-order SM (LOSM) equations are similar to those of the DSA method [8]. The main difference is that the LOSM equations are formulated for the angular moments of the solution, while the low-order DSA equations are defined for the iterative corrections of the moments. Thus, computational tools based on the DSA can be modified to use the SM method. We present a nonlinear multilevel SM (MLSM) method that consists of (i) multigroup high-order BTEs for group angular fluxes, (ii) multigroup LOSM equations for group scalar fluxes and currents, and (iii) grey LOSM equations for total scalar flux and current. The scattering terms in both group high-order and LOSM equations are formulated in a nonlinear form. The effective grey LOSM problem is defined by means of cross sections averaged with the iterative group LOSM solution. The group high-order BTEs and group LOSM equations are solved in parallel at corresponding stages of iteration algorithms. The group-to-group scattering terms in the group LOSM equations are defined with lagged iterative solution. In this case both downscattering and upscattering of particles have a similar effect on convergence of inner iterations with respect to energy groups. Iterations of this kind can yield slow convergence without acceleration. The convergence rate of inner iterations over the system of multigroup low-order equations is improved with use of the grey LOSM equations. To further accelerate convergence and increase computational efficiency of parallel algorithms we apply Anderson acceleration to the inner multigroup iterations [10].

The remainder of the paper is organized as follows. In Sec. 2, the MLSM method is formulated. In Sec. 3, we present the MLSM method with Anderson Acceleration of inner iterations over multigroup LOSM equations. The numerical results are presented in Sec. 4. We conclude with a discussion in Sec. 5.

## 2. Multilevel Second-Moment Method

We consider transport problems in 1D slab geometry. The iteration scheme of the MLSM method with groups solved in parallel is presented in Algorithm 1, where  $\ell$  is the index of outer transport iterations,  $k$  is the index of the inner iterations between multigroup and grey LOSM equations, and  $s$  is the index of the innermost iterations for solving multigroup LOSM equations.  $k_{max}$  and  $s_{max}$  are the maximum numbers of the corresponding inner iterations.

```

 $\ell = -1, \psi_g^{(0)} = \text{const}, P_g^{(0)} = 0, P^{(0)} = 0$ 
while  $\|\phi^{(\ell)} - \phi^{(\ell-1)}\| > \epsilon$  do
   $\ell = \ell + 1$ 
  if  $\ell > 0$  then
     $\phi_g^{(\ell-1)} \Rightarrow \bar{\sigma}_{s,g}^{(\ell-1)}, g \in \mathbb{G}$ 
    for all  $g \in \mathbb{G}$  in parallel do
      Level 1: Solve the high-order transport equation (Eqs. (2)) for group  $g$ 
       $\Rightarrow \psi_g^{(\ell)}$ 
     $\psi_g^{(\ell)} \Rightarrow P_g^{(\ell)}$  for  $g \in \mathbb{G}, P^{(\ell)}$ 
   $k = 0$ 
  while  $k \leq k_{max}$  do
     $k = k + 1$ 
     $s = 0$ 
    while  $s \leq s_{max}$  do
       $s = s + 1$ 
       $\phi_g^{(s-1,k,\ell)}, \phi^{(k-1,\ell)} \Rightarrow \zeta^{(s-1,k-1,\ell)}$ 
      for all  $g \in \mathbb{G}$  in parallel do
        Level 2: Solve the LOSM equation (Eqs. (3)) for group  $g \Rightarrow \phi_g^{(s,k,\ell)},$ 
         $J_g^{(s,k,\ell)}$ 
       $\phi_g^{(k,\ell)} \leftarrow \phi_g^{(s_{max},k,\ell)}, J_g^{(k,\ell)} \leftarrow J_g^{(s_{max},k,\ell)}$ 
       $\phi_g^{(k,\ell)}, J_g^{(k,\ell)} \Rightarrow \bar{\sigma}_a^{(k,\ell)}, \bar{\sigma}_t^{(k,\ell)}, \bar{\eta}^{(k,\ell)}$ 
      Level 3: Solve the grey LOSM equations (Eqs. (5))  $\Rightarrow \phi^{(k,\ell)}, J^{(k,\ell)}$ 
     $\phi_g^{(\ell)} \leftarrow \phi_g^{(k_{max},\ell)}, J_g^{(\ell)} \leftarrow J_g^{(k_{max},\ell)}, \phi^{(\ell)} \leftarrow \phi^{(k_{max},\ell)}, J^{(\ell+1)} \leftarrow J^{(k_{max},\ell)}$ 

```

**Algorithm 1:** The MLSM method with group equations solved in parallel

The multilevel hierarchy of equations of the MLSM method is defined as follows.

- **Level 1.** The multigroup high-order transport equations with decoupled groups are given by

$$\mu \frac{\partial \psi_g^{(\ell)}}{\partial x} + \sigma_{t,g} \psi_g^{(\ell)} = \frac{1}{2} \bar{\sigma}_{s,g}^{(\ell-1)} \phi^{(\ell-1)} + \frac{1}{2} Q_g, \quad \text{where} \quad \bar{\sigma}_{s,g}^{(\ell-1)} = \frac{\sum_{g'=1}^G \sigma_{s,g' \rightarrow g} \phi_{g'}^{(\ell-1)}}{\sum_{g'=1}^G \phi_{g'}^{(\ell-1)}}. \quad (2)$$

The right-hand side (RHS) of the BTE is transformed by means of (i) the total scalar flux that is the solution of the grey LOSM problem and (ii) averaged cross section  $\bar{\sigma}_{s,g}$  defined with the group scalar fluxes obtained from the multigroup LOSM equations [9].

- **Level 2.** The multigroup LOSM equations are defined by

$$\frac{dJ_g^{(s,k,\ell)}}{dx} + \left( \sigma_{t,g} - \sigma_{s,g \rightarrow g} \right) \phi_g^{(s,k,\ell)} = \zeta^{(s-1,k-1,\ell)} \sum_{\substack{g'=1 \\ g' \neq g}}^G \sigma_{s,g' \rightarrow g} \phi_{g'}^{(s-1,k,\ell)} + Q_g, \quad (3a)$$

$$\frac{1}{3} \frac{d\phi_g^{(s,k,\ell)}}{dx} + \sigma_{t,g} J_g^{(s,k,\ell)} = \frac{dP_g^{(\ell)}}{dx}, \quad (3b)$$

where

$$\zeta^{(s-1,k-1,\ell)} = \frac{\phi^{(k-1,\ell)}}{\sum_{g'=1}^G \phi_{g'}^{(s-1,k,\ell)}}, \quad P_g^{(\ell)} = \int_{-1}^1 \left( \frac{1}{3} - \mu^2 \right) \psi_g^{(\ell)} d\mu. \quad (4)$$

The RHS of Eq. (3) is formulated using the multiplicative correction factor  $\zeta$  that is defined by the solution of the multigroup and grey LOSM equations [9, 11]. This form of the RHS introduces nonlinearity in the multigroup LOSM equations.

- **Level 3.** The grey LOSM equations have the following form:

$$\frac{dJ^{(k,\ell)}}{dx} + \bar{\sigma}_a^{(k,\ell)} \phi^{(k,\ell)} = Q, \quad (5a)$$

$$\frac{1}{3} \frac{d\phi^{(k,\ell)}}{dx} + \bar{\sigma}_t^{(k,\ell)} J^{(k,\ell)} + \bar{\eta}^{(k,\ell)} \phi^{(k,\ell)} = \frac{dP^{(\ell)}}{dx}, \quad (5b)$$

where

$$\bar{\sigma}_a^{(k,\ell)} = \frac{\sum_{g=1}^G \sigma_{a,g} \phi_g^{(k,\ell)}}{\sum_{g=1}^G \phi_g^{(k,\ell)}}, \quad \bar{\sigma}_t^{(k,\ell)} = \frac{\sum_{g=1}^G \sigma_{t,g} |J_g^{(k,\ell)}|}{\sum_{g=1}^G |J_g^{(k,\ell)}|}, \quad (6)$$

$$\bar{\eta}^{(k,\ell)} = \frac{\sum_{g=1}^G \left( \sigma_{t,g} - \bar{\sigma}_t \right) J_g^{(k,\ell)}}{\sum_{g=1}^G \phi_g^{(k,\ell)}}, \quad P^{(\ell)} = \sum_{g=1}^G P_g^{(\ell)}, \quad Q = \sum_{g=1}^G Q_g. \quad (7)$$

The high-order BTE (Eq. (2)) is discretized by the linear-discontinuous (LD) finite element method. The spatial discretization of the multigroup and grey LOSM equations are consistent with the LD transport scheme [12].

### 3. The MLSM Method with Anderson Acceleration

#### 3.1. Anderson Acceleration

Let us consider a general equation of the following form:

$$\varphi = \mathcal{A}(\varphi), \quad \varphi \in \mathbb{R}^n \quad (8)$$

that is solved with the fixed-point iterations (FPI)

$$\varphi^{(s+1)} = \mathcal{A}(\varphi^{(s)}). \quad (9)$$

The residual for the  $s^{\text{th}}$  iterate  $\boldsymbol{\varphi}^{(s)}$  is defined by

$$\mathbf{r}(\boldsymbol{\varphi}^{(s)}) = \mathcal{A}(\boldsymbol{\varphi}^{(s)}) - \boldsymbol{\varphi}^{(s)}. \quad (10)$$

Anderson acceleration is an iterative algorithm that applies an extrapolation based on a linear combination of iterates and the values of  $\mathcal{A}$ . The coefficients of the linear combination are determined in such a way that they minimize the linear combination of the corresponding sequence of residuals. Algorithm 2 presents the iteration scheme of Anderson acceleration [10, 13, 14]. The parameter  $m$  defines the maximum algorithmic depth. The set of mixing parameters  $\beta_s$  are used for relaxation. We refer to this iteration algorithm as AA( $m$ ).

Define  $\boldsymbol{\varphi}^{(0)}$

$$\boldsymbol{\varphi}^{(1)} = \mathcal{A}(\boldsymbol{\varphi}^{(0)}), \quad \mathbf{r}(\boldsymbol{\varphi}^{(0)}) = \mathcal{A}(\boldsymbol{\varphi}^{(0)}) - \boldsymbol{\varphi}^{(0)}$$

**for**  $s = 1, 2, \dots$  **do**

$$\left[ \begin{array}{l} m_s = \min(m, s) \\ \mathbf{r}(\boldsymbol{\varphi}^{(s)}) = \mathcal{A}(\boldsymbol{\varphi}^{(s)}) - \boldsymbol{\varphi}^{(s)} \\ \min_{\boldsymbol{\alpha}^s} \left\| \sum_{j=0}^{m_s} \alpha_j^s \mathbf{r}(\boldsymbol{\varphi}^{(s-m_s+j)}) \right\|_2 \quad \text{s. t.} \quad \sum_{j=0}^{m_s} \alpha_j^s = 1. \\ \boldsymbol{\varphi}^{(s+1)} = (1 - \beta_s) \sum_{j=0}^{m_s} \alpha_j^s \boldsymbol{\varphi}^{(s-m_s+j)} + \beta_s \sum_{j=0}^{m_s} \alpha_j^s \mathcal{A}(\boldsymbol{\varphi}^{(s-m_s+j)}) \end{array} \right.$$

**Algorithm 2:** Anderson acceleration method for solving  $\boldsymbol{\varphi} = \mathcal{A}(\boldsymbol{\varphi})$

In this study, we use AA(1) with  $\beta_s = 1$  that converges r-linearly in  $\ell_2$ -norm provided that the coefficients  $\alpha_j^s$  are bounded [14]. This scheme defines the next iterate as follows:

$$\boldsymbol{\varphi}^{(s+1)} = \alpha_0^s \mathcal{A}(\boldsymbol{\varphi}^{(s-1)}) + \alpha_1^s \mathcal{A}(\boldsymbol{\varphi}^{(s)}) = \alpha_0^s \boldsymbol{\varphi}^{(s-1)} + \alpha_1^s \boldsymbol{\varphi}^{(s)} + \alpha_0^s \mathbf{r}(\boldsymbol{\varphi}^{(s-1)}) + \alpha_1^s \mathbf{r}(\boldsymbol{\varphi}^{(s)}), \quad (11)$$

where  $\boldsymbol{\alpha}^s = (\alpha_0^s, \alpha_1^s)^\top$  solves

$$\min_{\boldsymbol{\alpha}^s} \left\| \alpha_0^s \mathbf{r}(\boldsymbol{\varphi}^{(s-1)}) + \alpha_1^s \mathbf{r}(\boldsymbol{\varphi}^{(s)}) \right\|_2 \quad \text{s. t.} \quad \alpha_0^s + \alpha_1^s = 1. \quad (12)$$

To determine  $\alpha_0^s$ , we apply the following condition:

$$\left( \left\| \mathbf{r}(\boldsymbol{\varphi}^{(s)}) + \alpha_0^s (\mathbf{r}(\boldsymbol{\varphi}^{(s-1)}) - \mathbf{r}(\boldsymbol{\varphi}^{(s)})) \right\|_2^2 \right)'_{\alpha_0} = 0. \quad (13)$$

This yields

$$\alpha_0^s = \frac{\sum_{i=1}^n r_i^{(s)} (r_i^{(s)} - r_i^{(s-1)})}{\sum_{i=1}^n (r_i^{(s-1)} - r_i^{(s)})^2}, \quad (14)$$

where  $\{r_i^{(s)}\}_{i=1}^n = \{r_i(\boldsymbol{\varphi}^{(s)})\}_{i=1}^n$ .

### 3.2. MLSM Algorithm with Anderson Acceleration of Innermost Iterations

We apply AA(1) to the inner iterations of the multigroup LOSM equations at Level 2 (see Sec. 2). The vector of the solution  $\boldsymbol{\varphi} = \{\boldsymbol{\varphi}_g\}_{g=1}^G$  consists of  $\boldsymbol{\varphi}_g$  defined by the grid functions of  $\phi_g$  and  $J_g$ . The residual is given by  $\mathbf{r}(\boldsymbol{\varphi}) = \{\mathbf{r}_g\}_{g=1}^G$ , where  $\mathbf{r}_g(\boldsymbol{\varphi}) = \mathcal{F}_g \boldsymbol{\varphi}$  and  $\mathcal{F}_g$  is the operator of the discretized LOSM equations in the group  $g$ . The iteration scheme for the MLSM method with AA(1) for the inner multigroup iterations is presented in Algorithm 3. Hereafter we refer to this algorithm as the MLSM-AA(1) method.

...

$k = 0, \phi_g^{(0,\ell)} = \int_{-1}^1 \psi_g^{(\ell)} d\mu, J_g^{(0,\ell)} = \int_{-1}^1 \mu \psi_g^{(\ell)} d\mu$

**while**  $k \leq k_{max}$  **do**

$k = k + 1, s = 0$

$\hat{\phi}_g^{(0,k,\ell)} = \phi_g^{(k-1,\ell)}, \hat{J}_g^{(0,k,\ell)} = J_g^{(k-1,\ell)}, \phi_g^{(0,k,\ell)} = \phi_g^{(k-1,\ell)}$

Calculate residual  $\mathbf{r}(\hat{\varphi}^{(0,k,\ell)})$  of the multigroup LOSM equations

**while**  $s \leq s_{max}$  **do**

$s = s + 1$

$\phi_g^{(s-1,k,\ell)}, \phi^{(k-1,\ell)} \Rightarrow \zeta^{(s-1,k-1,\ell)}$

**for all**  $g \in \mathbb{G}$  **in parallel do**

Level 2: Solve the LOSM equation for group  $g \Rightarrow \hat{\phi}_g^{(s,k,\ell)}, \hat{J}_g^{(s,k,\ell)}$

Calculate residual  $\mathbf{r}(\hat{\varphi}^{(s,k,\ell+1)})$  of the multigroup LOSM equations

$\mathbf{r}(\hat{\varphi}^{(s,k,\ell)}), \mathbf{r}(\hat{\varphi}^{(s-1,k,\ell)}) \Rightarrow \alpha_0, \alpha_1$

$\varphi^{(s,k,\ell)} = \alpha_0 \hat{\varphi}^{(s-1,k,\ell)} + \alpha_1 \hat{\varphi}^{(s,k,\ell)} + \alpha_0 \mathbf{r}(\hat{\varphi}^{(s-1,k,\ell)}) + \alpha_1 \mathbf{r}(\hat{\varphi}^{(s,k,\ell)})$

$\varphi^{(s,k,\ell)} \Rightarrow \phi_g^{(s,k,\ell)}, J_g^{(s,k,\ell)}$

...

...

**Algorithm 3:** The MLSM-AA(1) method with group equations solved in parallel.

#### 4. Numerical Results

**Test 1.** This is a 10-group problem for a slab  $0 \leq x \leq 32$  [6]. The cross sections are given in Table A.6 (see Appendix A). The groups are coupled with each other due to downscattering and upscattering. The boundary conditions are vacuum. The external source is constant and  $Q_g = 1 \forall g$ . The spatial mesh is uniform with 128 cells. There are 16 angular directions. The double  $S_8$  Gauss-Legendre quadrature set is used. The convergence criterion is  $\varepsilon = 10^{-9}$ . Table 1 shows the measure of connection strength of groups given by [15]

$$S_{gg'} = \frac{a_{gg'}}{\max_{g'' \neq g} (a_{gg''})}, \quad a_{gg'} = \sigma_{s,g' \rightarrow g}. \quad (15)$$

In this test, most of groups are strongly connected with other groups. The group scattering is high and in the range  $0.9 \leq c_g \leq 0.9999$  (see Table A.6). The target number of transport iterations in Test 1 equals 15.

Table 2 shows the numbers of outer transport iterations ( $N_t$ ) and numerically estimated spectral radii ( $\rho_{num}$ ) for the MLSM and MLSM-AA(1) methods based on the rates of convergence during last iterations. The residual histories for the methods are presented in Figures 1a. The Fourier analysis in continuous form yields that the value of theoretical spectral radius (for an infinite-medium problem) of source iterations (SI) in this test is  $\rho_{th}^{SI} = 0.96$ . The full DSA (FDSA) method has  $\rho_{th}^{FDSA} = 0.21$  [6]. The study of the grey DSA (GDSA) and decoupled DSA (DDSA) showed that in this problem  $\rho_{num}^{GDSA} = 0.55$  and  $\rho_{num}^{DDSA} = 0.26$

Table 1: Connection strength of groups ( $S_{gg'}$ ) in Test 1

$g \setminus g'$	1	2	3	4	5	6	7	8	9	10
1	0	0	0	0	0	0	0	0	0	0
2	1.	0	0	0	0	0	0	0	0	0
3	0.71	1.	0	0	0	0	0	0	0	0
4	1.	0.53	0.36	0	0	0	0	0	0	0
5	1.	0.21	0.48	1.	0	0	0	0	0	0
6	0	0.78	0.64	1.	0.81	0	0	0	0	0
7	0	0	0.26	0.09	0.20	0.48	0	1.	0.22	0.23
8	0	0	0	0.91	0.11	0.25	0.13	0	1.	0.88
9	0	0	0	0	0.39	0.29	1.	0.78	0	0.62
10	0	0	0	0	0	0.41	1.	0.55	0.68	0

Table 2: Test 1

method	MLSM			MLSM-AA(1)	
$k_{max}$	1		2	1	
$s_{max}$	1	2	1	1	2
$N_t$	16	15	15	15	15
$\rho_{num}$	0.20	0.20	0.19	0.20	0.20
$M_{lo}$	2	3	4	2	3

[6].

On each transport iteration, the MLSM algorithm executes  $k_{max}s_{max}$  parallel solves of LOSM equations in groups and  $k_{max}$  solves of grey LOSM equations. Thus, it performs  $M_{lo} = k_{max}(s_{max} + 1)$  low-order solves where each solve of group LOSM equations is accounted as one because of parallel execution of groups. This measure can be used to evaluate the algorithm efficiency for the given number of transport iterations.

The results show that MLSM with  $k_{max} = 1$  and  $s_{max} = 1$  converges fast. Just one extra cycle over group LOSM equations ( $s_{max} = 2$ ) leads to the target number of transport iterations ( $N_t = 15$ ). The estimated spectral radius of this algorithm is  $\rho_{num} = 0.2$ . This version of the algorithm has the smaller number of cycles of low-order solves ( $M_{lo} = 3$ ) compared to the algorithm with  $k_{max} = 2$  and  $s_{max} = 1$ . The MLSM-AA(1) method slightly improves convergence in this test. This algorithm with  $k_{max} = 1$  and  $s_{max} = 1$  shows the best performance in this test. It converges in  $N_t = 15$  requiring  $M_{lo} = 2$ .

**Test 2.** This problem is similar to Test 1. It is defined with the moderator material from C5G7 benchmark with 7-group cross sections [16]. Table A.7 shows the cross section (see Appendix A). The connection strength of groups is presented in Table 3. The groups are strongly connected to neighbouring groups. The connection to distant groups is very weak. The group scattering is very high in all groups ( $0.985949 \leq c_g \leq 0.999961$ ). The target number of outer transport iterations is equal to 15.

Table 3: Connection strength of groups ( $S_{gg'}$ ) in Test 2

$g \setminus g'$	1	2	3	4	5	6	7
1	0	0	0	0	0	0	0
2	1.	0	0	0	0	0	0
3	$5.5 \times 10^{-3}$	1.	0	0	0	0	0
4	$1.7 \times 10^{-5}$	$2.8 \times 10^{-3}$	1.	0	$3.2 \times 10^{-4}$	0	0
5	$1.3 \times 10^{-7}$	$1.2 \times 10^{-4}$	$4.1 \times 10^{-2}$	1.	0	$5.3 \times 10^{-3}$	0
6	0	$1.5 \times 10^{-5}$	$5.2 \times 10^{-3}$	$1.3 \times 10^{-1}$	1.	0	$2.6 \times 10^{-1}$
7	0	$2.0 \times 10^{-6}$	$9.4 \times 10^{-4}$	$2.3 \times 10^{-2}$	$1.1 \times 10^{-1}$	1.	0

Table 4: Test 2: MLSM

$k_{max}$	1						2				3			4		5
$s_{max}$	1	2	3	4	5	6	1	2	3	4	1	2	3	1	2	1
$N_t$	31	26	22	20	18	18	26	20	16	15	22	16	15	20	15	15
$\rho_{num}$	0.45	0.38	0.31	0.28	0.22	0.26	0.38	0.29	0.22	0.20	0.33	0.22	0.20	0.29	0.20	0.20
$M_{lo}$	2	3	4	5	6	7	4	6	8	10	6	9	12	8	12	10

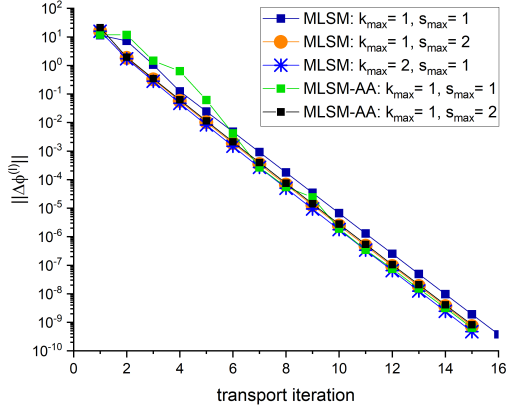
Table 5: Test 2: MLSM-AA(1)

$k_{max}$	1			2		3
$s_{max}$	1	2	3	1	2	1
$N_t$	31	18	17	18	15	15
$\rho_{num}$	n/a	0.27	0.26	n/a	0.20	0.20
$M_{lo}$	2	3	4	4	6	6

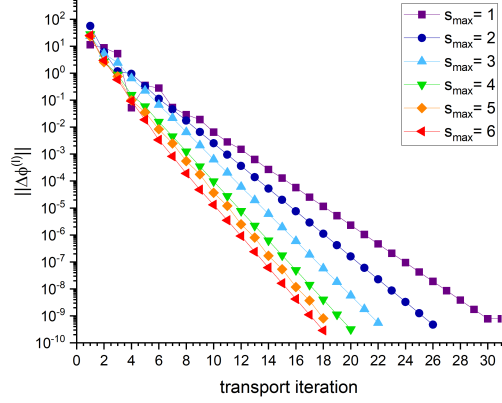
The numbers of outer transport iterations and numerically estimated spectral radii for the MLSM and MLSM-AA(1) methods are listed in Tables 4 and 5, respectively. The residual histories for both methods are presented in Figures 1b-1d. The theoretical spectral radii of SI and FDSA are  $\rho_{th}^{SI} = 0.98$  and  $\rho_{th}^{FDSA} = 0.22$ , respectively. The analysis of GDSA and DDSA showed that in this problem  $\rho_{num}^{GDSA} = 0.67$  and  $\rho_{num}^{DDSA} = 0.32$  [6].

The results show that the MLSM algorithm with  $k_{max} = 2$  and  $s_{max} = 4$  converges in  $N_t = 15$  requiring  $M_{lo} = 10$  per transport iteration. This method with  $k_{max} = 5$  with only  $s_{max} = 1$  also converges in  $N_t = 15$  and needs the same number  $M_{lo}$  per transport iteration. Application of Anderson acceleration significantly affects permeance of the MLSM method in this test. The most efficient is the MLSM-AA(1) algorithm with  $k_{max} = 2$  and  $s_{max} = 3$  that executes  $M_{lo} = 6$  per transport iteration. This algorithm converges steadily with estimated spectral radius  $\rho_{num} = 0.20$ . We note that the MLSM-AA(1) method with  $k_{max} = 1$  and  $s_{max} = 1$  showed irregular convergence behavior. This is the effect of using in Anderson acceleration just one residual of the solution of the group LOSM equations for  $s = 1$  and the residual of the initial guess ( $s = 0$ ) that is the high-order solution from the transport sweep.

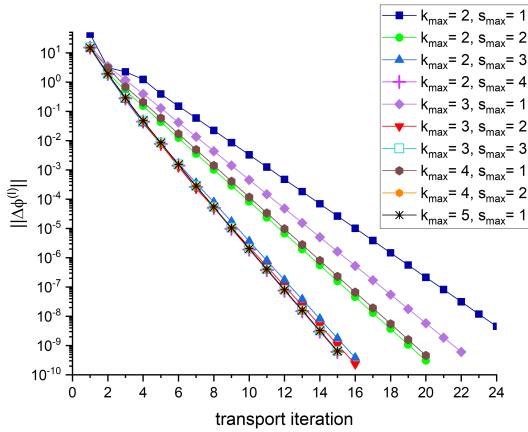




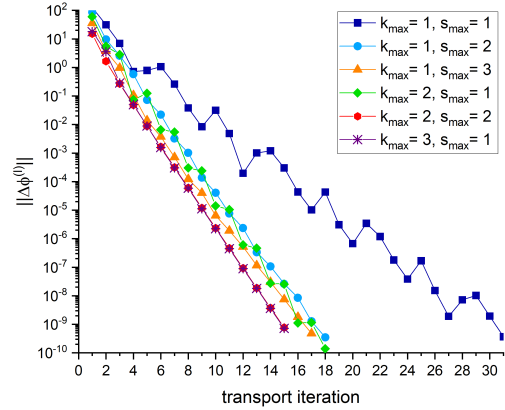
(a) Test 1



(b) Test 2, MLSM,  $k_{max} = 1$



(c) Test 2, MLSM,  $k_{max} = 2, 3, 4, 5$



(d) Test 2, MLSM-AA(1),  $k_{max} = 1, 2, 3$

Figure 1: Residual histories.

The trace of this effect can be also noticed in convergence behaviour of the MLSM-AA(1) method with  $k_{max} = 2$  and  $s_{max} = 1$ .

## 5. Conclusions

We developed new multilevel iterative methods for fixed-source multigroup particle transport problems that can be applied for parallel computations. Numerical results are promising. They show that the algorithms accelerate iterative convergence and effectively solve multigroup test problems with down- and upscattering as well as with high scattering ratios in groups. More analysis is needed to study properties of MLSM iterative algorithms. Further work will include extension to multi-D geometries and application of more general

version of Anderson acceleration. This kind of transport algorithms for parallel computations can also be developed on the basis of the quasidiffusion (VEF) method [9, 12].

## Acknowledgements

Los Alamos Report LA-UR-20-26669. This work was funded in part by Los Alamos National Laboratory, which is operated by Triad National Security, LLC, for the National Nuclear Security Administration of U.S. Department of Energy (Contract No. 89233218NCA000001). The work of the second author (JMC) was funded by LANL through a summer research internship in the CCS-2 group.

## References

- [1] J. E. Morel, E. W. Larsen, M. K. Matzen, A synthetic acceleration scheme for radiative diffusion calculations, *J. Quant. Spectrosc. Radiat. Transfer* 34 (1985) 243–261.
- [2] E. W. Larsen, A grey transport acceleration method for time-dependent radiative transfer problems, *Journal of Computational Physics* 78 (1988) 459–480.
- [3] J. E. Morel, T.-Y. B. Yang, J. S. Warsa, Linear multifrequency-grey acceleration recast for preconditioned Krylov iterations, *Journal of Computational Physics* 227 (2007) 244–263.
- [4] M. Hanus, J. Ragusa, Improving the performance of transport sweeps with thermal upscattering acceleration at massively parallel scale, in: *Int. Conf. on Mathematics and Computational Methods Applied to Nuclear Science and Engineering (M&C 2019)*, Portland, OR, August 25, 2019, pp. 475–484.
- [5] M. P. Adams, M. L. Adams, W. D. Hawkins, T. Smith, L. Rauchwerger, N. M. Amato, T. S. Bailey, R. D. Falgout, A. Kunen, P. Brown, Provably optimal parallel transport sweeps on semi-structured grids, *Journal of Computational Physics* 407 (2020) 109234.
- [6] J. S. Warsa, J. M. Coale, D. Y. Anistratov and J. H. Chang, Variations on diffusion-based synthetic acceleration for multigroup  $s_n$ , in: *Int. Conf. on Math. and Comp. Methods Applied to Nucl. Sci. and Eng., M&C 2021*, Raleigh, NC, October 2021.
- [7] E. Lewis, W. Miller, Jr., A comparison of  $p_1$  synthetic acceleration techniques, *Trans. Am. Nucl. Soc.* 23 (1976) 202.
- [8] M. L. Adams, E. W. Larsen, Fast iterative methods for discrete-ordinates particle transport calculations, *Progress in Nucl. Energy* 40 (2002) 1–159.
- [9] D. Y. Anistratov, V. Ya. Gol’din, Multilevel quasidiffusion methods for solving multigroup transport k-eigenvalue problems in one-dimensional slab geometry, *Nuclear Science and Engineering* 169 (2011) 111 – 132.
- [10] D. G. Anderson, Iterative procedures for nonlinear integral equations, *J. Assoc. Comput. Machinery* 12 (1965) 547–560.
- [11] D. Y. Anistratov, L. R. Cornejo, J. P. Jones, Stability analysis of nonlinear two-grid method for multigroup neutron diffusion problems, *Journal of Computational Physics* 346 (2017) 278–294.
- [12] D. Y. Anistratov, J. S. Warsa, Discontinuous finite element quasidiffusion methods, *Nuclear Science and Engineering* 191 (2018) 105–120.
- [13] H. Walker, P. Ni, Anderson acceleration for fixed-point iterations, *SIAM J. Numerical Analysis* 49 (2011) 1715–1735.
- [14] A. Toth, C. T. Kelley, Convergence analysis for Anderson acceleration, *SIAM J. Numerical Analysis* 53 (2015) 805–819.
- [15] W. L. Briggs, V. E. Henson, S. F. McCormick, *A multigrid tutorial*, SIAM, 2000.
- [16] E. E. Lewis, M. A. Smith, N. Tsoulfanidis, G. Palmiotti, T. A. Taiwo, R. N. Blomquist, Benchmark specification for deterministic 2-D/3-D MOX fuel assembly transport calculations without spatial homogenization (C5G7), *Expert Group on 3-D Radiation Transport Benchmarks NEA/NSC/DOC(2001)4* (2001).

## Appendix A. Cross Section Data

Table A.6: Cross section data for Test 1 [6]

$g$	1	2	3	4	5	6	7	8	9	10
$\sigma_{t,g}$	2.49756	2.01650	1.51992	1.67388	2.36661	1.50008	2.37543	2.36241	2.04640	1.59740
$c_g$	0.979581	0.944816	0.952295	0.926035	0.978471	0.9	0.987210	0.9999	0.904252	0.966192
$\tilde{g}$	$\sigma_{s,1\rightarrow\tilde{g}}$	$\sigma_{s,2\rightarrow\tilde{g}}$	$\sigma_{s,3\rightarrow\tilde{g}}$	$\sigma_{s,4\rightarrow\tilde{g}}$	$\sigma_{s,5\rightarrow\tilde{g}}$	$\sigma_{s,6\rightarrow\tilde{g}}$	$\sigma_{s,7\rightarrow\tilde{g}}$	$\sigma_{s,8\rightarrow\tilde{g}}$	$\sigma_{s,9\rightarrow\tilde{g}}$	$\sigma_{s,10\rightarrow\tilde{g}}$
1	0.835282	0	0	0	0	0	0	0	0	0
2	0.401686	0.566521	0	0	0	0	0	0	0	0
3	0.404298	0.569454	0.420634	0	0	0	0	0	0	0
4	0.498922	0.264139	0.179242	0.0828011	0	0	0	0	0	0
5	0.306376	0.0657747	0.148397	0.307318	1.30088	0	0	0	0	0
6	0.439338	0.362807	0.564376	0.456018	0.0715262	0	0	0	0	0
7	0	0	0.336331	0.122044	0.259295	0.623241	0.812409	1.28728	0.278371	0.301517
8	0	0	0	0.473528	0.0566290	0.128925	0.0676741	0.123057	0.518149	0.457140
9	0	0	0	0	0.242843	0.180473	0.622078	0.485474	0.483321	0.386770
10	0	0	0	0	0	0.345904	0.842890	0.466367	0.570623	0.397965

Table A.7: Cross section data for Test 2 [16]

$g$	1	2	3	4	5	6	7
$\sigma_{t,g}$	0.159206	0.412970	0.590310	0.584350	0.718000	1.25445	2.65038
$c_g$	0.996225	0.999961	0.999429	0.996679	0.992003	0.988042	0.985949
$\tilde{g}$	$\sigma_{s,1\rightarrow\tilde{g}}$	$\sigma_{s,2\rightarrow\tilde{g}}$	$\sigma_{s,3\rightarrow\tilde{g}}$	$\sigma_{s,4\rightarrow\tilde{g}}$	$\sigma_{s,5\rightarrow\tilde{g}}$	$\sigma_{s,6\rightarrow\tilde{g}}$	$\sigma_{s,7\rightarrow\tilde{g}}$
1	$4.44777\times 10^{-2}$	0	0	0	0	0	0
2	$1.134\times 10^{-1}$	$2.82334\times 10^{-1}$	0	0	0	0	0
3	$7.2347\times 10^{-4}$	$1.2994\times 10^{-1}$	$3.45256\times 10^{-1}$	0	0	0	0
4	$3.7499\times 10^{-6}$	$6.234\times 10^{-4}$	$2.2457\times 10^{-1}$	$9.10284\times 10^{-2}$	$7.1437\times 10^{-5}$	0	0
5	$5.3184\times 10^{-8}$	$4.8002\times 10^{-5}$	$1.6999\times 10^{-2}$	$4.1551\times 10^{-1}$	$1.39138\times 10^{-1}$	$2.2157\times 10^{-3}$	0
6	0	$7.4486\times 10^{-6}$	$2.6443\times 10^{-3}$	$6.3732\times 10^{-2}$	$5.1182\times 10^{-1}$	$6.99913\times 10^{-1}$	$1.3244\times 10^{-1}$
7	0	$1.0455\times 10^{-6}$	$5.0344\times 10^{-4}$	$1.2139\times 10^{-2}$	$6.1229\times 10^{-2}$	$5.3732\times 10^{-1}$	2.4807